Acta Oceanol. Sin., 2020, Vol. 39, No. 12, P. 54–64
https://doi.org/10.1007/s13131-020-1606-0
http://www.hyxb.org.cn
E-mail: hyxbe@263.net

Combining otolith elemental signatures with multivariate analytical models to verify the migratory pattern of Japanese Spanish mackerel (*Scomberomorus niphonius*) in the southern Yellow Sea

Xindong Pan[1], Zhenjiang Ye[1], Binduo Xu[1], Tao Jiang[2], Jian Yang[2], Jiahua Cheng[3], Yongjun Tian[1, 4, 5*]

[1] Fisheries College, Ocean University of China, Qingdao 266003, China

[2] Key Laboratory of Ecological Environment and Resources of Inland Fisheries, Freshwater Fisheries Research Center, Chinese Academy of Fishery Sciences, Wuxi 214081, China

[3] East China Sea Fishery Research Institute, Chinese Academy of Fishery Sciences, Shanghai 200090, China

[4] Laboratory for Marine Fisheries Science and Food Production Processes, Pilot National Laboratory for Marine Science and Technology (Qingdao), Qingdao 266071, China

[5] Frontiers Science Center for Deep Ocean Multispheres and Earth System, Ocean University of China, Qingdao 266100, China

Received 1 October 2019; accepted 18 March 2020

© Chinese Society for Oceanography and Springer-Verlag GmbH Germany, part of Springer Nature 2020

Abstract

Japanese Spanish mackerel, *Scomberomorus niphonius*, is a commercially important, highly migratory species that is widely distributed throughout the northwestern Pacific region. However, its life history and migratory patterns are only partially understood. This study used otolith chemistry to investigate the migratory pattern of *S. niphonius* in the southern Yellow Sea, an important fishing ground. Transverse sections of otoliths from 15 age-1 spawning or spent individuals, comprising up to one complete migration cycle, were analyzed from the core to the margin by using laser ablation inductively coupled plasma mass spectrometry. The ratios of the element to Ca were integrated with microstructural analysis to produce age-related elemental profiles. Combining multi-elemental analysis of otolith composition with multivariate analytical models, we quantified structural changes in otolith chemistry profiles. Results revealed there were diverse changing patterns of otolith chemistry profiles for detected elements and the elements of Na, Mg, Sr and Ba were important for the chronological signal. Five clusters were identified through chronological clustering, representing the five life stages from the early stage to the spawning stage. Variation of Ba:Ca ratio was most informative, showing a step-decreasing pattern in the first four stages and a rebound in the spawning stage. These results support the hypothesized migratory pattern of *S. niphonius*: hatching and spending their early life in the coastal sandy ridges system of the southern Yellow Sea, migrating northeastward and offshore for feeding during juvenile stage, aggregating in early October and migrating outward to the Jeju Island for wintering, and returning to the coastal waters for spawning. This study demonstrated the value of life-history related otolith chemistry profiles combined with multivariate analytical models was a means to verify the migration patterns of *S. niphonius* at regional scales with potential application in fisheries assessment and management.

Key words: otolith chemistry, *Scomberomorus niphonius*, migratory pattern, multivariate regression tree, southern Yellow Sea

Citation: Pan Xindong, Ye Zhenjiang, Xu Binduo, Jiang Tao, Yang Jian, Cheng Jiahua, Tian Yongjun. 2020. Combining otolith elemental signatures with multivariate analytical models to verify the migratory pattern of Japanese Spanish mackerel (*Scomberomorus niphonius*) in the southern Yellow Sea. Acta Oceanologica Sinica, 39(12): 54–64, doi: 10.1007/s13131-020-1606-0

1 Introduction

To investigate fish migration, one significant phenotypic approach developed over the past 20 years is the analysis of otolith chemistry (Campana, 1999; Elsdon and Gillanders, 2004; Elsdon et al., 2008; Sturrock et al., 2012) and it is an efficient and useful tool for tracking the migration paths. This approach is based on the reconstruction of environmental histories as recorded in the layering of the otolith (Sturrock et al., 2012; Walther and Limburg, 2012). Otolith chemistry works particularly well for these fishes associated with habitats of different water chemistries such as estuaries and rivers (Elsdon et al., 2008; Elsdon and Gillanders, 2003; Yang et al., 2006). To provide temporal records of movement between riverine, estuarine, and open sea environments, studies of diadramous fish mainly rely on the widely acceptable link between otolith Sr:Ca and ambient salinity (Elsdon et al., 2008; Elsdon and Gillanders, 2003; Yang et al., 2006). However, a meta-analysis on Sr:Ca assimilation into otoliths revealed that Sr:Ca incorporation in marine species is more likely to be physiological in nature (Brown and Severin, 2009). Therefore, for marine species, it is not enough to reconstruct the life-history migration merely based on the mono-elemental ap-

Foundation item: The National Natural Science Foundation of China under contract Nos 41930534 and 41876177.
*Corresponding author, E-mail: yjtian@ouc.edu.cn

proach (Sr:Ca). The modern use of laser ablation and microprobe analysis allows for multi-elemental analysis of otoliths and provides elemental compositions that are likely to be peculiar fingerprints for the water masses inhabited by fish (Chittaro et al., 2006). In addition to Sr, some other elements can also supply complementary information and can even be used as indicators for migration (Gemperline et al., 2002; Gillanders and Kingsford, 2003; Hicks et al., 2010; Jiang et al., 2016). As a result, multi-elemental approaches may be useful for understanding *S. niphonius* migration

Conventional studies of otolith chemistry are qualitative, consisting of visual interpretation of elemental transects through an otolith section, which could be subjective (Hedger et al., 2008; Walther and Limburg, 2012). Quantitative approaches to investigating fish movement patterns with otolith chemistry are desirable. However, only few are available. Fablet et al. (2007) reconstructed individual life histories from otolith chemical measures based on a signal-processing issue embedded in a Bayesian framework. Hedger et al. (2008) employed three zoning algorithms separately to quantitatively classify Sr:Ca otolith sequences into fish environmental histories. Thibault et al. (2010) employed a quantitative approach based on nonparametric smoothing (generalized additive models using penalised regression splines) to describe the otolith elemental transects. More recently, Vignon (2015) proposed a recursive partitioning method based on multivariate regression trees (MRT) to realize chronological clustering on the multi-elemental compositional otolith transect. Compared with the former three approaches, Vignon's method is easily interpretable and directly applicable to the detection of hidden discontinuities in any multivariate time series (Vignon, 2015). Other advantages are that there is no requirement for distributional assumptions and data transformations on the predictor and response variables (De'ath, 2002) and it is fully unsupervised thus avoiding any *priori* judgement on the expected patterns. In addition, it provides a powerful exploratory tool for assessing the relative importance of cross-correlated variables in structuring the environmental histories. This can help identify less useful elements in the multi-proxy context.

Japanese Spanish mackerel *Scomberomorus niphonius*, an epipelagic predator within the family *Scombridae*, is highly migratory and widely distributed in the temperate waters of the northwestern North Pacific Ocean (Qiu and Ye, 1996; Horikawa et al., 2001; Shoji and Tanaka, 2005). *Scomberomorus niphonius* is also a commercially important species in the adjacent sea areas of China, particularly in the southern Yellow Sea which is an important fishing ground. *Scomberomorus niphonius* is a repeat spawner whose pelagic eggs hatch in 54 h. Their larvae are piscivorous at first feeding and can swim freely to prey upon small fishes 5–6 d after hatching (Horikawa et al., 2001; Shoji and Tanaka, 2005). Rapid growth at a mean growth rate of 1.03 mm/d reduces the duration of larval stage to about 15 d (Horikawa et al., 2001; Shoji and Tanaka, 2005). Schooling behavior of mackerel juveniles is initiated from day 17 and completed by day 19, during which they start aggregation by forming parallel orientation indicating inception of migration behavior (Masuda et al., 2003). High feeding intensity of the young enables *S. niphonius* to achieve fast growth during the growing season of juveniles. Individuals of *S. niphonius* at smaller sizes consume small fishes such as anchovy (*Engraulis japonicus*), sand lance (*Ammodytes personatus*) and crustaceans but increasingly shifted to larger prey items such as chub mackerel (*Scomber japonicus*) and saury (*Cololabis saira*) as they grew larger (Huh et al., 2006).

Preliminary studies related to the migration of *S. niphonius* were carried out decades ago partially based on indirect inferences from fishing vessels data (Wei, 1980; Liu and Yang, 1982). These studies stated that *S. niphonius* undertook long-distance seasonal migrations. The species has been observed to move into shallow waters during warmer seasons to breed and spawn, then move back to deeper waters in the cooler seasons. Mature adults of this species in the southern Yellow Sea come from the overwintering grounds in the deep waters of the southeastern Yellow Sea and northeastern East China Sea. *Scomberomorus. niphonius* was reported to start its wintering migration in the late autumn and successively move to its wintering ground, for overwintering in January and February (Yuan et al., 2009; Kim et al., 2016). Every year after overwintering in February, *S. niphonius* would leave their wintering ground to start their spawning migration (Yuan et al., 2009). However, relevant studies have observed a regime shift in fish community (Tian et al., 2006) and a structural change in the *S. niphonius* population (Zhang et al., 2016; Shui et al., 2009). Additionally, after the late 1990s, the distribution, migration and fishing grounds of *S. niphonius* presented northward extension (Fujiwara et al., 2013). Given these phenomena, whether the previous migratory pattern is still convincing need to be verified. Furthermore, more comprehensive interpretation and reinforced evidence of the migratory pattern of *S. niphonius* based on the novel methods are also imperative.

In this study, we focused on the migratory pattern of *S. niphonius* from a regional stock, using samples collected from the southern Yellow Sea. Since *S. niphonius* is a fully marine species, we not only focus on Sr but using multi-elemental analysis of otoliths and combined with multivariate analytical models to identify important elements associated with apparent shifts in the data. It is difficult to establish link between environmental parameters (salinity, temperature, water chemistry) and each single element, as the mechanisms of elemental incorporation at the growing surface of the otolith are not fully understood (Elsdon et al., 2008). Nevertheless, such elemental shifts must either be directly related to regional differences in ambient water concentrations, water temperature and salinity or indirectly to the influence of these abiotic factors on the physiology of *S. niphonius*. Based on the understanding of *S. niphonius* life history and the oceanographic conditions in this area, those shifts which imply the quantitatively captured multivariate nature of structural changes in our data were associated to the important events such as metamorphosis and reproduction happened in the life history of fish. This process helps us to identify important elements associated with apparent shifts in the data and nominate the possible explanatory factors, enabling us to achieve biological interpretation of chemical signals and understand the migration pattern of *S. niphonius* in the southern Yellow Sea.

2 Materials and methods

2.1 *Sample collection*

Scomberomorus niphonius were randomly sampled from catches by commercial gill net vessels (mesh size 90–110 mm) operating in May 2016 in the Lüsi fishing ground of the southern Yellow Sea (Fig. 1). All sampled specimens were refrigerated immediately and transported to the laboratory. Fork length and body weight were measured to the nearest 1 mm and 1 g, respectively. Sex and maturity were determined through visual gonad examination for each sample (Inoue et al., 2007). Sagittal otoliths were extracted through the gill, cleaned in ultrapure water and then dried in the air prior to store in plastic tubes. Age was determined by counting the number of annuli in the otolith (Inoue et al., 2007). A total of 15 age-1 individuals in spawning or spent condition (Table 1) were selected for elemental analysis.

Scomberomorus niphonius reaches sexual maturity at one year old (Qiu and Ye, 1996) and the life history of these adults covered one complete migration cycle.

2.2 *Otolith preparation*

One whole sagitta was selected at random from each fish. It was embedded separately in epoxy resin (Epofix, Struers, Denmark), sectioned to approximately 400 μm in thickness in the transverse section-plane to encompass the core. The sections were ground with 500#, 1 200# grit paper and polished using an aluminium micropolisher (0.3 μm) with an automated polishing wheel (Roto Pol-35, Struers, Denmark) to expose the core. Thereafter, all samples were sonicated in an ultrasonic bath for 5 min and rinsed with Milli-Q water (Millipore, France). After decontamination, all samples were oven-dried at 38°C overnight for chemical analysis.

2.3 *Elemental analysis*

Laser ablation inductively coupled plasma mass spectrometry (LA-ICP-MS, Laser: New Wave UP213, ICP-MS: Agilent 7500ce) was used to obtain time-related element, Ca, profiles. The elemental analysis was conducted in the Key Laboratory of Ecological Environment and Resources of Inland Fisheries, Freshwater Fisheries Research Center, Chinese Academy of Fishery Sciences. The laser was programmed at a wave length of 213 nm, high voltage of 10 kV, pulse rate of 10 Hz, energy density of 9.29 J/cm^2 and a dwell time of 5 s. Ablation spots of 40 μm diameter were located at 80 μm intervals (from center to center) along the longest transect from the otolith core to the dorsal-distal edge. This axis was chosen for two reasons: (1) it was one of the clearest for differentiating the opaque zones for ontogenetic otolith elemental signature; (2) being a short axis, it minimized the deviation of the distance from the core to the edge for samples with roughly similar life span such that the number of detected spots narrowly ranged from 17 to 21. Sample gases were extracted from the chamber through a smoothing manifold facilitated by a helium and argon stream. Two standard samples NIST612 and MACS-3 (National Institute of Standards and Technology, USA; United States Geological Survey, USA) were analyzed at the beginning and end of the sampling sessions with 5 samples. Analysis involved a 100 s background count at the beginning and at the end to determine the actual limits of detection (LODs); relative standard deviations (RSD) on the basis of replicated measurements of the standard samples were calculated to

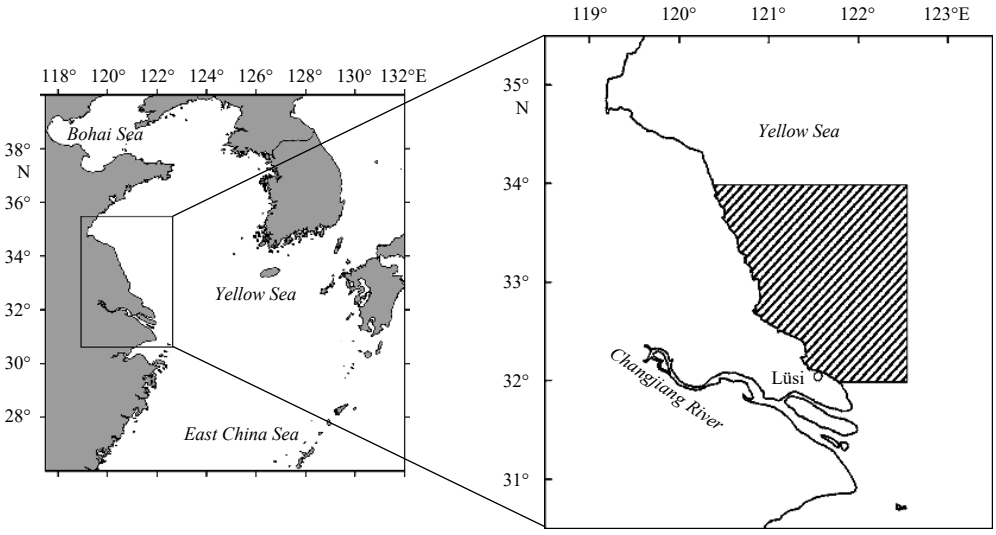

Fig. 1. Sampling locations (slashed area) of *S. niphonius* in the southern Yellow Sea.

Table 1. Background information of *S. niphonius* individuals for otolith chemistry analysis

Sample code	Sampling date (year/month/day)	Fork length/mm	Body mass/g	Age/a	Male (M)/female (F)
LSSN01	2016/5/8	466	883	1	F
LSSN02	2016/5/8	458	758	1	M
LSSN03	2016/5/8	462	869	1	F
LSSN04	2016/5/8	554	1 411	1	M
LSSN05	2016/5/14	440	663	1	F
LSSN06	2016/5/14	446	652	1	M
LSSN07	2016/5/14	406	533	1	M
LSSN08	2016/5/14	432	747	1	M
LSSN09	2016/5/14	464	807	1	F
LSSN10	2016/5/14	465	794	1	M
LSSN11	2016/5/14	430	621	1	M
LSSN12	2016/5/14	520	1 041	1	F
LSSN13	2016/5/14	509	1 030	1	M
LSSN14	2016/5/14	510	1 131	1	F
LSSN15	2016/5/14	525	1 149	1	F

reflect the level of precision achieved for each element. All results were expressed as concentration ratios of elements to calcium (Amano et al., 2013). Of all the measures, LODs for Li (0.503 μmol/mol), Na (3.25 μmol/mol), Mg (0.552 μmol/mol), Fe (167 μmol/mol), Co (0.102 μmol/mol), Sr (0 μmol/mol) and Ba (0.018 5 μmol/mol) were all well below the detected radio in otoliths. The analytical accuracy of the standard across all samples was high for all elements with RSD ranging from 2.87% to 5.55% (Li: 4.73%, Na: 2.87%, Mg: 5.55%, Fe: 3.58%, Co: 5.09%, Sr: 4.36%, Ba: 5.53%).

2.4 *Microstructural analysis to relate elemental profile to fish age*

Digital photographs were taken for these otolith sections after LA-ICP-MS analysis (Fig. 2) and the distance of each laser ablation spot relative to the otolith core was expressed as distance from their center to the first spot center (0 μm). The otolith of *S. niphonius* begins to form in the postembryonic period. Marginal increment analysis performed by Liu and Yang (1982) and Inoue et al. (2007) on different stocks both determined that opaque zones were formed over a period of three months after spawning. Sagittal otolith increments of *S. niphonius* are deposited daily in the larval and early juvenile periods (Shoji et al., 1999). The microstructure analysis performed on otolith sections clarified that the core region was formed in the first 9–10 d with a width about 40 μm. The opaque zones surrounding the core were formed immediately in the following 15–20 d and the microincrements get broader to about 10 μm in average. The translucent zones with radial striae after it were formed in the subsequent remaining period. In the spawning season the mircoincrements grew progressively closer to each other and often became faint. Given the different growing speed in different periods of the otolith, to allow for more straightforward comprehension of life history transect data with a life span covering roughly one year's time, we related the elemental profile to the fish life history following three steps: (1) the first spot in the core region was determined as representing the first 10 d of fish life history; (2) the following three spots in the first opaque zone were allocated evenly with a time interval of 15 d; (3) the remaining spots in the translucent or the marginal opaque zones were equally designated to each represent a period of 20 d. An otolith growth model would have provided a direct method for spacing spots to get a time-resolved elemental profile. However, in the absence of such a model for *S. niphonius*, this procedure was judged as providing the most realistic representation of different stages in fish life history corresponding to each analytical measurement.

2.5 *Data analysis*

Since each spot corresponds to a time period of *S. niphonius* growth, the elemental values of spots were grouped to obtain the chronological data series within an individual. All detected elements can be used as inputs to a traditional tree-based approach to detect chronological groups in multivariate data. However, on no occasion were all elements of a data series useful; even worse, some elements may complicate or cover up the signal in the data, thereby precluding clear portioning. Therefore, it is of top priority to disentangle the relative importance of different elements in structuring the data in order to discard the most unstructured elements (Vignon, 2015).

Three most well-known and well-performing techniques are available to estimate the relative importance, including boosting, bagging (bootstrap aggregating) and random forest (Mercier et al., 2011). Here we have chosen to use random forest, an ensemble machine learning algorithm, which determines the contribution of each variable by measuring the number of times a variable is selected for splitting, weighted by the squared improvement to the model as a result of each split, and averaged over all trees (De'ath, 2002). For our study, we used a tree number of 1 000 and a bagging fraction of 0.7. The relative importance (or contribution) of each variable is scaled so that the sum adds to 100, with a higher number indicating stronger influence on the chronological clustering. The threshold of the important variable was set as being greater than 10% of the relative importance. To investigate the inter-individual variation in element importance, a principal coordinates analysis (PCoA, also known as metric multidimensional scaling) was used in two dimensions (Gower, 1966). A Euclidean distance measure for each pair of matrices was used as input for metric multidimensional scaling. The resulting principal coordinates are axes that account for the maximum amount of the information contained in the corresponding distance matrix. Such an ordination allows one to visualize the relationship among matrices. If two matrices are close in the PCO (principal coordinates) plane, they are correlated and have similar relative importance of elements.

A multivariate regression tree (MRT) model is developed for the multivariate chronological clustering based on the elements selected as being important. MRT (De'ath, 2002) constructs a hierarchical tree by recursive binary (dichotomies) partitioning (nodes) into two mutually exclusive groups ('the leaves of MRT'), each of which is as homogeneous as possible and the final tree size was determined with cross-validation error (Breiman et al., 1984). Recently, Borcard et al. (2011) suggested that MRT could easily be applied to multivariate chronological clustering, using a vector describing the sequence as the only explanatory variable. The final MRT model was based on the scaled elemental ratios since we were interested in relative variations in different elements, not in their absolute value. If data are not scaled, it is likely that the discontinuities obtained from the regression tree correlate with changes in the variable that has the largest variation in magnitude, irrespective of other variables (Vignon, 2015).

All statistical analyses were carried out in R (R Development Core Team, 2013; version 3.3.3). Models were fitted using the new functions from the R package Tampo that depends on packages Mvpart and Randomforest. Additional information can be obtained at http://www6.bordeaux-aquitaine.inra.fr/st_pee/UMR-Ecobiop/Outils/TAMPO/TAMPO. An up-to-date version of the R package *Tampo* and its future development are hosted on GitHub (http://github.com/mvignon).

Fig. 2. Image of a transverse section of an *S. niphonius* otolith showing the laser ablation spots.

3 Results

3.1 *Life-history related otolith chemistry profiles*

Otoliths from 15 age-1 spawned *S. niphonius* captured in the southern Yellow Sea were successfully analyzed, and 288 detected spots were obtained with a maximum of 21 in one otolith. Elemental ratios (Li:Ca, Na:Ca, Mg:Ca, Fe:Ca, Co:Ca, Sr:Ca and Ba:Ca) in mackerel otoliths are shown in Table 2. The composition of these elements showed that Na was the highest, Fe the second and Li, Co and Ba the lowest.

Diverse patterns of life-history related otolith chemistry profiles were present for these 7 elements (Fig. 3). The mean estimates of Li:Ca ranged from 2.22 μmol/mol to 4.11 μmol/mol (Fig. 3a). A slightly decreasing pattern after 300 d was observed in the Li:Ca profile. Mean estimates of Na:Ca ranged from 8 222.66 μmol/mol to 10 960.06 μmol/mol (Fig. 3b). The Na:Ca ratio declined rapidly after Day 200. Mg:Ca and Ba:Ca showed very similar patterns with a predominantly declining trend and an increase in the final days (Figs 3c, g) with mean levels ranging from 99.27 μmol/mol to 355.32 μmol/mol and from 2.19 μmol/mol to 5.83 μmol/mol, respectively. Small ranges and variations were found both in the Fe:Ca (7 398.61–8 011.37 μmol/mol) and Co:Ca (5.24–6.16 μmol/mol) profiles (Figs 3d, e). The mean estimates of Sr:Ca ranged from 1 986.96 μmol/mol to 2 761.83 μmol/mol (Fig. 3f). The Sr:Ca profile remained stable for the first 240 d but fluctuated more drastically afterwards.

3.2 *Relative importance of the elements in the chronological signal*

The multi-elemental analysis based on random forest results from 15 individual fish reveals sharp contrasts among the elements regarding their influence in the signal (Fig. 4). Among all elements used in the analyses, only 4 were important (Fig. 4), which were then used to analyze migration patterns. The chemical profiles from the otoliths of all fishes are predominantly structured by variations in Mg and Ba. In addition, Sr and Na also appear to be important but at a significantly lesser extent. In contrast, Li, Fe and Co are not important (all having a mean relative influence less than 10%, Fig. 4), providing more noise than signal with respect to environmental histories, and are therefore of little interest.

PCoA reveals that inter-individual variation in element importance mainly relies on Mg (first component accounting for 57% of total variability, Fig. 5). The PCoA results also indicate that Ba, having a similar pattern to that of Mg, also structures the signal and is likely to be an important element for analysis of the migration pattern. Sr and Na, as the third and fourth most important elements of the structure signals, highlighted the potential complementarity between elemental signals. In addition, results for most individuals converged on the central zone of the PCO plane, suggesting that they had similar patterns of relative importance for all elements.

3.3 *Multivariate chronological clustering*

The final MRT model was based on the scaled Na:Ca, Mg:Ca, Sr:Ca and Ba:Ca ratios (Fig. 6). On the condition of optimal cross-validation error, four splits were detected at the distance of 800 μm, 1 200 μm, 240 μm and 1 040 μm sequentially which divided the time series data into five clusters. The model explains 53% of the total variance.

A summary of the number of detected spots, represented age period and elemental radio for each cluster is provided in Table 3. Cluster 1 was distinguished as the beginning period with four data spots included and characterized with high levels of Na:Ca, Mg:Ca, Sr:Ca and Ba:Ca. Cluster 2 represented a long age period after that with seven data spots included. During this time period, Mg:Ca, Sr:Ca and Ba:Ca were all decreasing to a lower level when compared to Cluster 1. The following days were represented by Cluster 3 with three data spots included, which was characterized by even lower levels of Mg:Ca and Ba:Ca and by the lowest level of Sr:Ca. A short time period with two data spots was represented by Cluster 4, with the discriminatory feature that levels of Na:Ca, Mg:Ca and Ba:Ca were all at the lowest levels. Cluster 5 represented the final days including five data spots and was characterized by the highest Sr:Ca level. In general, the variations of Na:Ca and Sr:Ca levels among the five clusters were both limited. Na:Ca levels were lower in Clusters 4 and 5, and Cluster 5 had the highest Sr:Ca level. Mg:Ca and Ba:Ca levels both showed steep decreasing pattern from Cluster 1 to Cluster 4 but increased in Cluster 5.

4 Discussion

Effective management of *S. niphonius* in the adjacent sea areas of China requires knowledge of population structure, connectivity, migration patterns of spawning aggregations, and distribution in a changing climate. However, the partial understanding of the life history pattern and the complex population structure of *S. niphonius* in the adjacent sea areas of China has hampered effective management (Zhang et al., 2016; Shui et al., 2009). This study evaluated the use of otolith chemistry signatures combined with multivariate analytical models as a means to reconstruct the migration patterns of *S. niphonius* in the southern Yellow Sea. Our results revealed diverse changing patterns of life-history related otolith chemistry profiles in detected elements and found that Na, Mg, Sr and Ba were important and most informative to the structure of the chronological signal. An MRT model based on important elements resulted in five clusters through the chronological clustering. On the theoretical basis that otolith signatures vary according to the physicochemical properties of the ambient environment (Campana, 1999; Elsdon et al., 2008), the given set of elemental radio of these clusters reflected five specific habitats in which *S. niphonius* operated during their migration cycle. Thus, by understanding and integrating the life history, historical migratory pattern, and further spatio-temporal resolution of the piecewise signal, our study has verificated the migratory pattern of *S. niphonius* and raised a hypothesized migratory pattern of the *S. niphonius* in the southern Yellow Sea.

4.1 *Temporal resolving of otolith chemistry signal*

Provided with the understanding of the life history of *S. niphonius*, the time periods represented by our clusters could be

Table 2. The summary of elements ratios (μmol/mol) in the otolith for all *S. niphonius* samples

	Li:Ca	Na:Ca	Mg:Ca	Fe:Ca	Co:Ca	Sr:Ca	Ba:Ca
Mean value	3.61	9 819.62	186.33	7 765.30	5.74	2 190.31	3.78
SD value	1.49	1 438.52	122.54	964.49	0.99	439.57	2.46
Min value	1.28	6 212.26	54.93	5 400.82	3.83	1 320.94	1.00
Max value	11.14	14 419.08	958.22	12 163.79	11.05	4 480.77	16.82

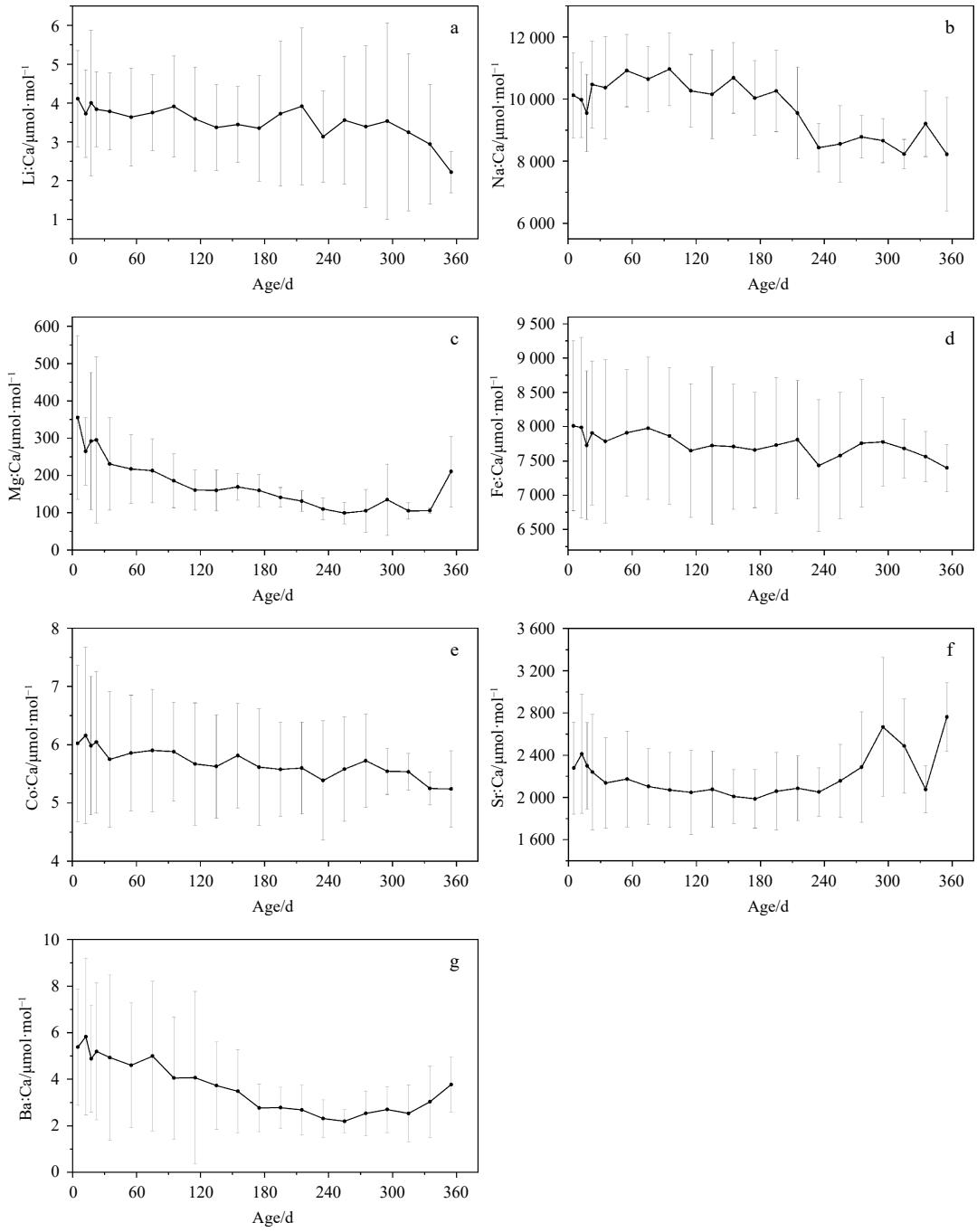

Fig. 3. Patterns of life-history related otolith chemistry profiles. The dots are the mean value of data spots and error bars are standard errors.

defined as different life stages in the ontogeny. The time period of Cluster 1 corresponded to the early life history from embryonic development, hatching, to the larval and juvenile stages. Hence, we defined Cluster 1 as the early stage with mackerel inhabiting in its zone of natal origin. The time period of Cluster 2 was roughly from summer to autumn, corresponding to a growing season. *Scomberomorus niphonius* is expected to be highly migratory as it forages and Cluster 2 can be defined as the feeding (migration) stage. The wintering migration started in the late autumn and overwintering stage was in January and Febuary. This corresponded to the time periods represented by Cluster 3 and Cluster 4, from October to late January; these two clusters represented the wintering migration and overwintering stages, respectively. Over 90% of *S. niphonius* matured at Age 1 and age-1 individuals constituted a large portion of annual landings (Qiu and Ye, 1996), likely induced by intensive fishing over an extended period. The time period of Cluster 5 correlated with this spawning stage at which young *S. niphonius* migrated to their spawning ground, became sexually mature, and ultimately completed the migration cycle of their life history by laying eggs. This temporal interpretation was based on our relating of elemental profiles to fish life history; however, the present result may suffer from the methodological problems that may be attributed to the equally-spaced designation of detected spots in the translucent and the

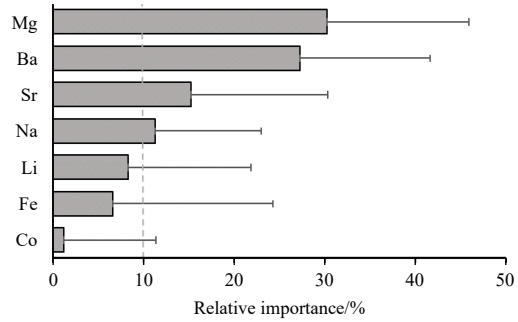

Fig. 4. Mean relative importance±SD of 7 elements in structuring the multivariate signal using the random forest model. The relative importance of each variable is scaled so that the sum adds to 100. A threshold of 10% (vertical dotted line) was used to identify elements of importance.

marginal opaque zones. Since otolith growth rate decreases exponentially with time (Liu and Yang, 1982), this method may have caused the time period of each cluster to be slightly in advance of the time period it truly represented.

Chronological clusters were temporally resolved as five life stages: the early stage, the feeding stage, the wintering migration stage, the overwintering stage and the spawning stage. The split between the wintering migration and overwintering stages seemed to be attributed to the sharply decreasing trend of Na:Ca (Fig. 7). Na is a physiologically important element (Kalish, 1991; Thresher et al., 1994) and fluctuates not with the environment but with the osmoregulatory control (Campana, 1999). Given that the high-low step change in Na:Ca profile merely reflected the peculiar intrinsic process when *S. niphonius* left their feeding ground for the wintering ground. The Na:Ca profile provided no information on the ambient environment. Sr:Ca levels peaked in the spawning stage and the different changing pattern after 240 d provided the basis for the split between the overwintering and the spawning stages (Fig. 7). Sr concentrations were often assumed to be positively correlated with the salinity in the ambient environment (Campana, 1999; Gillanders, 2005; Walther and Limburg, 2012), with the exception of some marine systems (Walther and Limburg, 2012). The narrow salinity gradients experienced by *S. niphonius* as a fully marine fish could explain the limited variations of Sr:Ca. However, physiological processes, particularly reproduction, may be outweighed in explaining the high Sr:Ca levels in the spawning stage, as documented in plaice (*Pleuronrctes platessa*) (Sturrock et al., 2015). Additional research is required to conclusively define whether Sr:Ca can be used as an indicator for the development of gonad in the marine environment. The step-changing pattern of Mg:Ca contributed significantly to all the four splits (Fig. 7). It is considerably more difficult to separate the effect of temperature and growth rate on the incorporation of Mg, as growth is generally strongly influenced by temperature (Kalish, 1991; Bath et al., 2000). We hypothesized that Mg:Ca in the otolith of *S. niphonius* is regulated simultaneously by growth rate and temperature, as Grammer et al. (2017) documented. From the early stage to the overwintering stage, the decline of Mg:Ca was probably driven by the decreasing growth rate, less so by the changes in water temperature as water temperature was not simply rising or dropping from spring to winter. However, Mg:Ca in the spawning stage was more likely to be elevated by the generally rising water temperature after winter when growth took a back seat. This piecewise synchrony of Mg, growth rate and water temperature suggested that the element incorporation could be dominated by different factors in different life stages.

Since physiology and environment both play a role in elemental incorporation into otoliths, chemical heterogeneity that we detected among individuals was not only a result of environ-

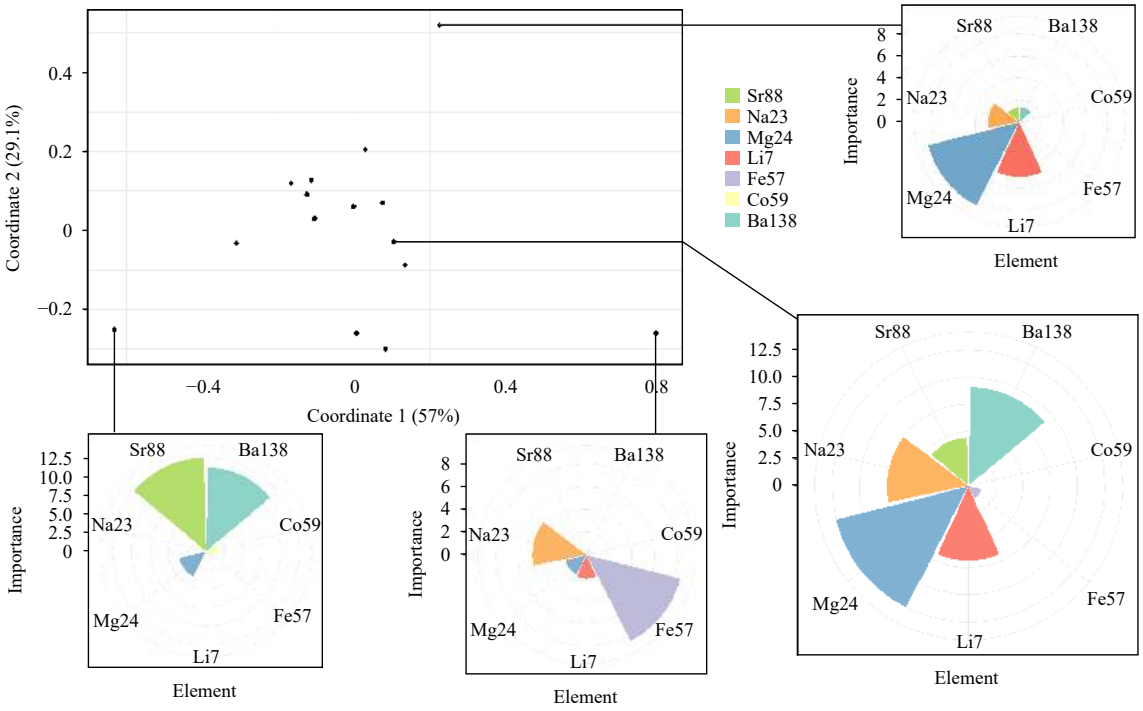

Fig. 5. PCoA depicting the inter-individual variation in element importance (based on the random forest model). Details are given for four individuals using polar barplots.

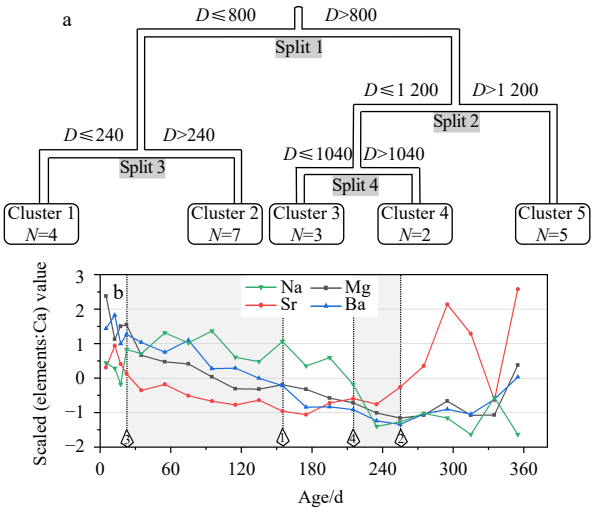

Fig. 6. Multivariate chronological clustering. a. Multivariate regression tree depicting the four splits and five clusters (*N* indicating the number of measures), numbered sequentially. For each partition, the threshold value is indicated (*D* indicating the distance to the nucleus). b. Life-history related original data (scaled) fitted with the corresponding MRT. The splits are numbered according to a.

mental effect but also attributed to the different physiological conditions of different samples, such as metabolic rate, growth rate, age and fish diet (Izzo et al., 2018). Thus, elemental data used to reconstruct migration pattern can be misinterpreted if physiology-induced changes in element concentrations are unaccounted for (Thresher, 1999; Elsdon et al., 2008; Sturrock et al., 2012). The synchrony among individuals may also reflect the aggregating movement of *S. niphonius* for wintering after the feeding stage during which the young tend to be dispersed in the extensive feeding ground to prey on small fish. The environmental homogeneity caused by the putative movement was more convincing in the Ba:Ca since Ba:Ca tend to be correlated with environment rather than physiological parameters (Sturrock et al., 2012, 2015).

Previous studies of otolith chemistry in reconstructing the migratory history and stock discrimination have used several kinds of elements (e.g. Li, Na, Mg, Zn, Sr, Ba, Mn, Pb, Fe, Cu, S) (Edmonds et al., 1991; Secor et al., 1995a, b; Campana, 1999; Campana and Thorrold, 2001; Thresher, 1999; Elsdon et al., 2008). In this study, we retained seven valid elements (without Ca) after LA-ICP-MS analysis that had quite different ranges and patterns of their life-history related otolith chemistry profiles. The concentrations of measured elements in our study were consistent with the observed mean concentration values in marine species (Campana, 1999) and they are showing variable changing patterns.

Table 3. The summary of distance, detected spots and elemental radio for each cluster

Cluster number	Distance/μm	Number of spots	Na:Ca/μmol·mol^{-1}		Mg:Ca/μmol·mol^{-1}		Sr:Ca/μmol·mol^{-1}		Ba:Ca/μmol·mol^{-1}	
			Mean	SD	Mean	SD	Mean	SD	Mean	SD
1	$D\leqslant240$	4	10 028.53	378.52	301.80	38.20	2 307.39	74.51	5.32	0.40
2	$240<D\leqslant800$	7	10 569.11	316.23	190.92	29.27	2 088.47	55.44	4.26	0.59
3	$800<D\leqslant1\,040$	3	9 945.78	364.13	144.04	14.51	2 044.25	51.54	2.74	0.05
4	$1\,040<D\leqslant1\,200$	2	8 495.82	84.31	104.65	7.61	2 104.42	75.02	2.25	0.08
5	$D>1\,200$	5	8 619.01	413.08	132.28	45.60	2 455.92	279.23	2.91	0.52

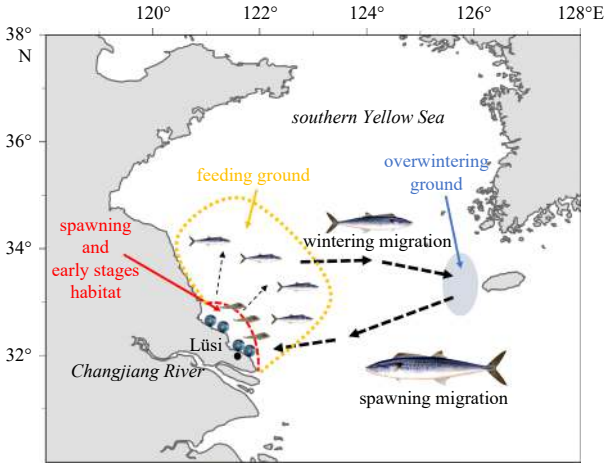

Fig. 7. A conceptual diagram showing the hypothesized life-history migration of the *S. niphonius* in the southern Yellow Sea.

We built our MRT model using the putative important elements of Na, Mg, Sr and Ba. However, this does not preclude the potential usage of other elements. For example, Li:Ca in the otolith was most strongly correlated (positive) with chlorophyll *a* levels in the environment and could be a potential indicator of productivity within the marine environment (Grammer et al., 2017). It was the poor ability of structuring chronological signal that caused us to exclude them in this study. PCoA analysis showed that most individuals in our study were correlated and had similar pattern of relative importance for all elements, which highlighted the chemical homogeneity among individuals and the feasibility of successful assignment of *S. niphonius* in different spawning aggregations using fingerprint data sets.

4.2 *Spatial resolving of otolith chemistry signal*

Na:Ca, Mg:Ca and Sr:Ca in our study were to some extent influenced by the physiology of *S. niphonius*. Nevertheless, Ba, as a typically hard acid element, exists mainly as a free ion in water and 98% of Ba in otolith of marine fish originated from water sources (Walther and Thorrold, 2006). Thus, Ba:Ca was primarily affected by environment parameters and the positive correlations with Ba concentrations in the ambient water have been well documented (Grammer et al., 2017; Sturrock et al., 2012). The peaked Ba:Ca in the early stage implied that the habitat during this period was characterized by high Ba concentration.

Variation in ambient water chemistry is likely to be system dependent, relating to tides, water movements, hydrogeology, precipitation, and upwelling (Elsdon et al., 2008). In the southern Yellow Sea, the shallow coastal regions located off the eastern coast of China between the Changjiang River Delta to the south and the abandoned Huanghe River Delta to the north is

composed of approximately 70 unique sandy ridges and associated tidal channels, at a mean water depth of approximately 30 m below mean sea level (Uehara and Saito, 2003; Yin et al., 2008). Obvious upwelling is observed in the coastal waters of Lüsi in the north and west sides of the submarine valley off the Changjiang River Estuary (Zhu et al., 2004; Lü et al., 2006). As the waters tend to be Ba enriched due to dissolution of barite in deep ocean water and sediments in strong upwelling areas (Lea and Boyle, 1991), the ambient Ba levels in the coastal sandy ridges seem to be higher than the other coastal waters or the offshore waters. There are some other complementary evidences for the higher ambient Ba in coastal sandy ridges. Typically, Ba:Ca ratios in nearshore marine carbonates display a negative correlation with salinity and can act as a proxy for coastal freshwater runoff (Chan et al., 2011). Every year from May to September, when the Changjiang Diluted Water runs out from the estuary, its main body extends northeastward and brings Ba-enriched freshwater inflows (Wei et al., 2011).

Additionally, the water mass transported by the Subei coastal current, the coastal current originated from the north Haizhou Bay to influence the sandy ridges, are of low salinity and carrying amount of resuspended sediments (including Ba) from the ancient Huanghe River Estuary underwater delta (Wei et al., 2011). Consequently, the coastal sandy ridges are probably the first habitat that impresses high otolith Ba:Ca signal in the core. Ba:Ca showed a step-declining pattern from the early stage to the overwintering stage which contributed significantly to the initial three splits (Fig. 7). It could be inferred that the following habitats were characterized by gradually decreasing Ba concentration. Since the ambient Ba concentrations in the coastal water was higher than the open sea and the Changjiang Diluted Water continued influencing the southwest area of the southern Yellow Sea in summer, the shifts of the habitat indicated that a large number of juvenile *S. niphonius* made a northeastward migration in the feeding stage, from the coastal sandy ridges to the offshore mixing area (the second habitat) with a water depth from 40 m to 60 m below mean sea level. Previous studies suggested that *S. niphonius* spawned in the southern Yellow Sea came from the wintering ground of the western and southwestern waters of the Jeju Island (32°00′–33°40′N, 124°40′–127°15′E), which was influenced by the high salinity west branch of the Tsushima Warm Current (Yuan et al., 2009). This was supported by the low otolith Ba:Ca in the overwintering stage in our study and suggested the eastward and outward wintering migration (the third habitat) of the young of the year to reach the wintering ground (the fourth habitat). Based on the resolving of these four life stages, it is quite clear that the recovery of the Ba:Ca in the spawning stage could be an indicator of the *S. niphonius* backtracking to the coastal waters of the Lüsi fishing ground (the fifth habitat), the sample site in this study.

4.3 *Reconstructing the migratory pattern of S. niphonius in the southern Yellow Sea*

After spatio-temporal resolving of otolith chemistry signal, verification of the migratory pattern of *S. niphonius* in the southern Yellow Sea showed no significant changes and difference from the putative migratory pattern based on conventional tag-recapture studies in 1964 (Zhang et al., 2013). The hypothesized migratory pattern of the *S. niphonius* in the southern Yellow Sea is showed in Fig. 7. *Scomberomorus niphonius* hatch and spend their early life in the coastal sandy ridges system of the southern Yellow Sea; their juveniles migrate northeastward around early June and disperse in the offshore mixing area for feeding. After fattening and conserving enough energy, the young begin aggregating in early October and migrate outward to reach the Jeju Island for wintering. The migration cycle is completed by returning to the coastal waters again for spawning.

Despite some limitations such as limited sample size and lacking water chemistry information, our results prove the feasibility of using otolith chemistry signatures combined with multivariate analytical models to identify important elements associated with apparent shifts in the data and to verify the migration pattern of *S. niphonius*. Through this process we can reconstruct the possible migratory pattern of *S. niphonius* more precisely and authoritatively, which could be a reinforced evidence for the inadequacy of simply using fisheries catch data for inferring migration. Good understanding of the life-history migration of *S. niphonius* does not only help to localize the fish assemblages on which fisheries rely, but also elucidates the connectivity between larval/juvenile sources and adult population, and this would be especially informative to management of this commercially important species. Based on the first step beginning with the southern Yellow Sea, future steps should include taking into consideration of other spawning aggregations along the China coastal waters and samples from former and later years to comprehensively investigate the migration pattern of this highly migratory species.

In spite of climate change and over-exploitation in the adjacent sea areas of China (Cheung et al., 2013; Liang and Pauly, 2017; Ma et al., 2019; Pang et al., 2018), *S. niphonius* supported a high yield over the past decades. The interdisciplinary approaches bring us brand new perspective to understand the life history of large-scale migratory species and the influence on regional population dynamics and stock structure. Making good use of the interdisciplinary approaches may help us to explain this phenomenon and establish effective and responsible management strategies. Besides, they can also be applying to other species to realize sustainable exploitation.

Acknowledgements

We thank all scientific staff and crew for their assistance with sample collection and experimental implementation. We thank Andrew Bakun (University of Miami) and Caihong Fu (Fisheries and Oceans Canada, Pacific Biological Station) for their valuable comments and proofreading.

References

Amano Y, Kuwahara M, Takahashi T, et al. 2013. Otolith elemental and Sr isotopic composition as a natal tag for Biwa salmon *Oncorhynchus masou* subsp. in Lake Biwa, Japan. Aquatic Biology, 19(1): 85–95, doi: 10.3354/ab00520

Bath G E, Thorrold S R, Jones C M, et al. 2000. Strontium and barium uptake in aragonitic otoliths of marine fish. Geochimica et Cosmochimica Acta, 64(10): 1705–1714, doi: 10.1016/S0016-7037(99)00419-6

Borcard D, Gillet F, Legendre P. 2011. Spatial analysis of ecological data. In: Borcard D, Gillet F, Legendre P, eds. Numerical Ecology with R. New York: Springer, 227–292

Breiman L, Friedman J H, Olshen R A, et al. 1984. Classification and regression trees. Biometrics, 40(3): 874

Brown R J, Severin K P. 2009. Otolith chemistry analyses indicate that water Sr:Ca is the primary factor influencing otolith Sr:Ca for freshwater and diadromous fish but not for marine fish. Canadian Journal of Fisheries and Aquatic Sciences, 66(10): 1790–1808, doi: 10.1139/F09-112

Campana S E. 1999. Chemistry and composition of fish otoliths: pathways, mechanisms and applications. Marine Ecology Progress

Series, 188: 263–297, doi: 10.3354/meps188263
Campana S E, Thorrold S R. 2001. Otoliths, increments, and elements: keys to a comprehensive understanding of fish populations?. Canadian Journal of Fisheries Aquatic Science, 58(1): 30–38, doi: 10.1139/f00-177
Chan P, Halfar J, Williams B, et al. 2011. Freshening of the Alaska Coastal Current recorded by coralline algal Ba/Ca ratios. Journal Geophysical Research: Biogeosciences, 116(G1): 1387–1387
Cheung W W, Watson R, Pauly D. 2013. Signature of ocean warming in global fisheries catch. Nature, 497(7449): 365–368, doi: 10.1038/nature12156
Chittaro P M, Usseglio P, Fryer B J, et al. 2006. Spatial variation in otolith chemistry of *Lutjanus apodus* at Turneffe Atoll, Belize. Estuarine, Coastal and Shelf Science, 67(4): 673–680, doi: 10.1016/j.ecss.2005.12.014
De'ath G. 2002. Multivariate regression trees: a new technique for modeling species-environment relationships. Ecology, 83(4): 1105–1117
Edmonds J S, Caputi N, Morita M. 1991. Stock discrimination by trace-element analysis of otoliths of Orange Roughy (*Hoplostethus atlanticus*), a deep-water marine teleost. Australian Journal of Marine and Freshwater Research, 42(4): 383–389, doi: 10.1071/MF9910383
Elsdon T S, Gillanders B M. 2003. Reconstructing migratory patterns of fish based on environmental influences on otolith chemistry. Reviews in Fish Biology and Fisheries, 13(3): 217–235, doi: 10.1023/B:RFBF.0000033071.73952.40
Elsdon T S, Gillanders B M. 2004. Fish otolith chemistry influenced by exposure to multiple environmental variables. Journal of Experimental Marine Biology and Ecology, 313(2): 269–284, doi: 10.1016/j.jembe.2004.08.010
Elsdon T S, Wells B K, Campana S E, et al. 2008. Otolith chemistry to describe movements and life-history parameters of fishes: hypotheses, assumptions, limitations and inferences. Oceanography and Marine Biology: An Annual Review, 46(1): 297–330
Fablet R, Daverat F, De Pontual H. 2007. Unsupervised Bayesian reconstruction of individual life histories from otolith signatures: case study of Sr:Ca transects of European eel (*Anguilla anguilla*) otoliths. Canadian Journal of Fisheries and Aquatic Sciences, 64(1): 152–165, doi: 10.1139/f06-173
Fujiwara K, Satou S, Tojima T, et al. 2013. Maturity and spawning of female Spanish mackerel *Scomberomorus niphonius* in the Sea of Japan. Bulletin of Kyoto Prefectural Agriculture (in Japanese), 25: 13–18
Gemperline P J, Rulifson R A, Paramore L. 2002. Multi-way analysis of trace elements in fish otoliths to track migratory patterns. Chemometrics and Intelligent Laboratory Systems, 58(1–2): 135–146
Gillanders B M. 2005. Otolith chemistry to determine movements of diadromous and freshwater fish. Aquatic Living Resources, 18(3): 291–300, doi: 10.1051/alr:2005033
Gillanders B M, Kingsford M J. 2003. Spatial variation in elemental composition of otoliths of three species of fish (family *Sparidae*). Estuarine, Coastal and Shelf Science, 57(5–6): 1049–1064
Gower J C. 1966. Some distance properties of latent root and vector methods used in multivariate analysis. Biometrika, 53(3–4): 325–338
Grammer G L, Morrongiello J R, Izzo C, et al. 2017. Coupling biogeochemical tracers with fish growth reveals physiological and environmental controls on otolith chemistry. Ecological Monographs, 87(3): 487–507, doi: 10.1002/ecm.1264
Hedger R D, Atkinson P M, Thibault I, et al. 2008. A quantitative approach for classifying fish otolith strontium: calcium sequences into environmental histories. Ecological Informatics, 3(3): 207–217, doi: 10.1016/j.ecoinf.2008.04.001
Hicks A S, Closs G P, Swearer S E. 2010. Otolith microchemistry of two amphidromous galaxiids across an experimental salinity gradient: a multi-element approach for tracking diadromous migrations. Journal of Experimental Marine Biology and Ecology, 394(1–2): 86–97
Horikawa H, Zheng Y, Meng T. 2001. Biological and Ecological Characteristics of Valuable Fisheries Resources from the East China Sea and the Yellow Sea—Comparison between the Chinese and Japanese Knowledge. Nagasaki, Japan: Seikai National Fisheries Research Institute
Huh S H, Park J M, Baeck G W. 2006. Feeding habits of spanish mackerel (*Scomberomorus niphonius*) in the southern sea of Korea. Korean Journal of Fisheries and Aquatic Sciences, 39(1): 35–41, doi: 10.5657/kfas.2006.39.1.035
Inoue T, Wada Y, Tojima T, et al. 2007. Age and migration of the Japanese Spanish Mackerel (*Scomberomorus niphonius*) in the coastal waters of Kyoto Prefecture. Bulletin of the Kyoto Institute of Oceanic & Fishery Science, 29: 1–6
Izzo C, Reis-Santos P, Gillanders B M. 2018. Otolith chemistry does not just reflect environmental conditions: A meta-analytic evaluation. Fish and Fisheries, 19(3): 441–454, doi: 10.1111/faf.12264
Jiang Tao, Liu Hongbo, Lu Mingjie, et al. 2016. A Possible connectivity among estuarine tapertail anchovy (*Coilia nasus*) populations in the Yangtze River, Yellow Sea, and Poyang Lake. Estuaries and Coasts, 39(6): 1762–1768, doi: 10.1007/s12237-016-0107-z
Kalish J M. 1991. Oxygen and carbon stable isotopes in the otoliths of wild and laboratory-reared Australian salmon (*Arripis trutta*). Marine Biology, 110(1): 37–47, doi: 10.1007/BF01313090
Kim H, Lim Y N, Song S H, et al. 2016. Understanding the migration path of Spanish mackerel *Scomberomorus niphonius* using catch distributions. Korean Journal of Fisheries and Aquatic Sciences, 49(3): 376–384, doi: 10.5657/KFAS.2016.0376
Lea D W, Boyle E A. 1991. Barium in planktonic foraminifera. Geochimica et Cosmochimica Acta, 55(11): 3321–3331, doi: 10.1016/0016-7037(91)90491-M
Liang Cui, Pauly D. 2017. Fisheries impacts on China's coastal ecosystems: Unmasking a pervasive 'fishing down' effect. PLoS One, 12(3): e0173296, doi: 10.1371/journal.pone.0173296
Liu Chanxin, Yang Kaiwen. 1982. Studies on the growth of Spanish mackerel, *Scomberomorus niphonius* in the Huanghai Sea and Bohai Sea. Oceanologia et Limnologia Sinica (in Chinese), 13(2): 170–178
Lü Xinguang, Qiao Fangli, Xia Changshui, et al. 2006. Upwelling off Yangtze River estuary in summer. Journal of Geophysical Research: Oceans, 111(C11): C11S08
Ma Shuyang, Cheng Jiahua, Li Jianchao, et al. 2019. Interannual to decadal variability in the catches of small pelagic fishes from China Seas and its responses to climatic regime shifts. Deep Sea Research Part II: Topical Studies in Oceanography, 159: 112–129, doi: 10.1016/j.dsr2.2018.10.005
Masuda R, Shoji J, Nakayama S, et al. 2003. Development of schooling behavior in Spanish mackerel *Scomberomorus niphonius* during early ontogeny. Fisheries Science, 69(4): 772–776, doi: 10.1046/j.1444-2906.2003.00685.x
Mercier L, Darnaude A M, Bruguier O, et al. 2011. Selecting statistical models and variable combinations for optimal classification using otolith microchemistry. Ecological Applications, 21(4): 1352–1364, doi: 10.1890/09-1887.1
Pang Yumeng, Tian Yongjun, Fu Caihong, et al. 2018. Variability of coastal cephalopods in overexploited China Seas under climate change with implications on fisheries management. Fisheries Research, 208: 22–33, doi: 10.1016/j.fishres.2018.07.004
Qiu Shengyao, Ye Maozhong. 1996. Studies on the reproductive biology of *Scomberomorus niphonius* in the Yellow Sea and Bohai Sea. Oceanologia et Limnologia Sinica (in Chinese), 27(5): 463–470
R Development Core Team. 2013. R: A language and environment for statistical computing. Vienna, Austria: R Foundation for Statistical Computing
Secor D H, Dean J M, Campana S E. 1995a. Recent Developments in Fish Otolith Research. Columbia, SC: University of South Carolina Press
Secor D H, Henderson-Arzapalo A, Piccoli P M. 1995b. Can otolith microchemistry chart patterns of migration and habitat utiliza-

tion in anadromous fishes?. Journal of Experimental Marine Biology and Ecology, 192(1): 15–33, doi: 10.1016/0022-0981(95)00054-U

Shoji J, Maehara T, Tanaka M. 1999. Short-term occurrence and rapid growth of Spanish mackerel larvae in the central waters of the Seto Inland Sea, Japan. Fishery Science, 65(1): 68–72, doi: 10.2331/fishsci.65.68

Shoji J, Tanaka M. 2005. Distribution, feeding condition, and growth of Japanese Spanish mackerel (*Scomberomorus niphonius*) larvae in the Seto Inland Sea. Fishery Bulletin, 103(2): 371–379

Shui Bonian, Han Zhiqiang, Gao Tianxiang, et al. 2009. Mitochondrial DNA variation in the East China Sea and Yellow Sea populations of Japanese Spanish mackerel *Scomberomorus niphonius*. Fisheries Science, 75(3): 593–600, doi: 10.1007/s12562-009-0083-3

Sturrock A M, Hunter E, Milton J A, et al. 2015. Quantifying physiological influences on otolith microchemistry. Methods in Ecology and Evolution, 6(7): 806–816, doi: 10.1111/2041-210X.12381

Sturrock A M, Trueman C N, Darnaude A M, et al. 2012. Can otolith elemental chemistry retrospectively track migrations in fully marine fishes?. Journal of Fish Biology, 81(2): 766–795, doi: 10.1111/j.1095-8649.2012.03372.x

Thibault I, Hedger R D, Dodson J J, et al. 2010. Anadromy and the dispersal of an invasive fish species (*Oncorhynchus mykiss*) in eastern Quebec, as revealed by otolith microchemistry. Ecology of Freshwater Fish, 19(3): 348–360, doi: 10.1111/j.1600-0633.2010.00417.x

Thresher R E. 1999. Elemental composition of otoliths as a stock delineator in fishes. Fisheries Research, 43(1–3): 165–204

Thresher R E, Proctor C, Gunn J S, et al. 1994. An evaluation of electron-probe microanalysis of otoliths for stock delineation and identification of nursery areas in a southern temperate groundfish, Nemadactylus macropterus (*Cheilodactylidae*). Fishery Bulletin, 92(4): 817–840

Tian Yongjun, Kidokoro H, Watanabe T. 2006. Long-term changes in the fish community structure from the Tsushima warm current region of the Japan/East Sea with an emphasis on the impacts of fishing and climate regime shift over the last four decades. Progress in Oceanography, 68(2–4): 217–237

Uehara K, Saito Y. 2003. Late Quaternary evolution of the Yellow/East China Sea tidal regime and its impacts on sediments dispersal and seafloor morphology. Sedimentary Geology, 162(1–2): 25–38

Vignon M. 2015. Extracting environmental histories from sclerochronological structures—Recursive partitioning as a mean to explore multi-elemental composition of fish otolith. Ecological Informatics, 30: 159–169, doi: 10.1016/j.ecoinf.2015.10.002

Walther B D, Limburg K E. 2012. The use of otolith chemistry to characterize diadromous migrations. Journal of Fish Biology, 81(2): 796–825, doi: 10.1111/j.1095-8649.2012.03371.x

Walther B D, Thorrold S R. 2006. Water, not food, contributes the majority of strontium and barium deposited in the otoliths of a marine fish. Marine Ecology Progress Series, 311: 125–130, doi: 10.3354/meps311125

Wei Sheng. 1980. The fishing seasons and grounds of the blue spotted mackerel, *Scomberomorus niphonius* in the Yellow Sea and Bohai in relation to environmental factors. Transaction of Oceanology and Limnology (in Chinese), (2): 34–40

Wei Qinsheng, Yu Zhigang, Ran Xiangbin, et al. 2011. Characteristics of the western coastal current of the Yellow Sea and its impacts on material transportation. Advances in Earth Science (in Chinese), 26(2): 145–156

Yang Jian, Arai T, Liu Hongbo, et al. 2006. Reconstructing habitat use of *Coilia mystus* and *Coilia ectenes* of the Yangtze River estuary, and of *Coilia ectenes* of Taihu Lake, based on otolith strontium and calcium. Journal of Fish Biology, 69(4): 1120–1135, doi: 10.1111/j.1095-8649.2006.01186.x

Yin Yong, Zou Xinqin, Zhu Dakui, et al. 2008. Sedimentary facies of the central part of radial tidal sand ridge system of the eastern China coast. Frontiers of Earth Science in China, 2(4): 408–417, doi: 10.1007/s11707-008-0053-6

Yuan Yangyang, Ye Zhenjiang, Liu Qun, et al. 2009. Fishery oceanography and spatial-temporal distribution of *Scomberomorus niphonius* in spring in southern Yellow Sea. Oceanologia et Limnologia Sinica (in Chinese), 40(4): 506–510

Zhang Chi, Ye Zhenjiang, Li Zengguang, et al. 2016. Population structure of Japanese Spanish mackerel *Scomberomorus niphonius* in the Bohai Sea, the Yellow Sea and the East China Sea: evidence from random forests based on otolith features. Fisheries Science, 82(2): 251–256, doi: 10.1007/s12562-016-0968-x

Zhang Chi, Ye Zhenjiang, Panhwar S K, et al. 2013. Stock discrimination of the Japanese Spanish mackerel (*Scomberomorus niphonius*) based on the otolith shape analysis in the Yellow Sea and Bohai Sea. Journal of Applied Ichthyology, 29(2): 368–373, doi: 10.1111/jai.12084

Zhu Jianrong, Qi Dingman, Wu Hui. 2004. Observation and modeling analysis of dynamic mechanism of the upwelling at Lusi. Journal of East China Normal University (Natural Science) (in Chinese), (2): 87–91, 103